International Journal of Materials Science and Applications
2016; 5(5): 222-227
http://www.sciencepublishinggroup.com/j/ijmsa
doi: 10.11648/j.ijmsa.20160505.17
ISSN: 2327-2635 (Print); ISSN: 2327-2643 (Online)

Surface Valence States of Mn Ions and Magnetic Properties of $La_{0.67}Sr_{0.33}MnO_3$ Films

Ruikun Pan*, Yang Li, Fan Fang, Wanqiang Cao

School of Materials Science & Engineering, Hubei University, Wuhan, China

Email address:

panruikun5@sina.com (Ruikun Pan)

*Corresponding author

To cite this article:

Ruikun Pan, Yang Li, Fan Fang, Wanqiang Cao. Surface Valence States of Mn Ions and Magnetic Properties of $La_{0.67}Sr_{0.33}MnO_3$ Films. *International Journal of Materials Science and Applications*. Vol. 5, No. 5, 2016, pp. 222-227. doi: 10.11648/j.ijmsa.20160505.17

Received: September 10, 2016; **Accepted**: October 7, 2016; **Published**: October 13, 2016

Abstract: $La_{0.67}Sr_{0.33}MnO_3$ (LSMO) films were prepared on $SrTiO_3$ single-crystal substrates by the pulsed laser deposition method. X-ray photoelectron spectra (XPS) were measured for the LSMO films as-prepared, annealed in oxygen and in vacuum, respectively. Multiple peaks fitting for Mn $2p_{3/2}$ XPS spectra shows that Mn^{2+} appears and the ratio of Mn^{3+}/Mn^{4+} increases on the surface of LSMO film annealed in vacuum comparing with the as-prepared film, though the saturation magnetization (M_s) changes little. Mn^{6+} and Mn^{7+} can be detected while Mn^{4+} decreases much on the surface of LSMO film annealed in oxygen. The change of Mn^{3+}/Mn^{4+} results in the obviously reduce of M_s. O1s spectra show the gradual changes of Mn-O, Sr-O and La-O. Analysis indicates that Mn^{2+} forms at the surface defects of LSMO films. Annealing in vacuum hardly affects the magnetic property of LSMO films. But annealing in oxygen greatly changes the valence states of Mn, which weakens the magnetic property of LSMO films.

Keywords: $La_{0.67}Sr_{0.33}MnO_3$ Film, XPS, Annealing, Magnetic Property

1. Introduction

Perovskite-like doped lanthanum manganite $La_{0.67}Sr_{0.33}MnO_3$ (LSMO) is a half-metallic material as its Curie temperature is higher than room temperature, which is very attractive for spintronics applications, e.g. ferroelectric tunnel junctions and all-oxide magneto-electric tunnel junction with LSMO films used as ferromagnetic electrodes [1-5]. Recently many reports focus on the interface structural and magnetic properties of LSMO films deposited on $SrTiO_3$ (STO) substrates [6-8].

After depositing films, annealing process always needs to improve the crystallization and remove some defects. Different annealing temperature, process time and atmosphere can lead to different results for the annealed films. D.R. Sahu et al. reported that $La_{0.7}Sr_{0.3}MnO_3$ thin film were annealed ex-situ at 1173 K and 1273 K temperatures in oxygen flow for 1 h, which improves the magnetic homogeneity of the grain and grain boundaries [9]. High annealing temperature even causes composition segregation. H.P. Xie et al. reported LaMnO*x* is formed due to strontium segregation on the surface at a temperature higher than 1023 K annealed in air for LSMO thin films [10]. But few studies have focused on the annealing process and the magnetic properties.

X-ray photoemission spectra (XPS) measurements of the core levels and valence electronic structure of Mn 2p in LSMO and other metal oxides have been reported in recent years [11-13]. Mn 2p XPS spectra of LSMO films are more complicated than those of bulk and free ions since Mn^{2+}, Mn^{3+} and Mn^{4+} can coexist on the surface or in the films [14, 15]. Multiple-peak fitting is always used to analyze the multiple splitting of Mn 2p spectra of Mn^{2+}, Mn^{3+} and Mn^{4+} ions. It should be mentioned that for each Mn ion, multiple peaks with various intensities can be got during the spectral fitting [11]. The intensity ratios of these multiple peaks of each ion in film materials may be changed from those of bulks due to the complexity and metastability of the film materials.

Here we prepared LSMO films by the pulsed laser deposition (PLD) method and fitted Mn $2p_{3/2}$ spectra. The intensity ratios of Mn^{2+}, Mn^{3+} and Mn^{4+} were changed with different annealing treatments, which have different effects on the magnetic properties of the LSMO films. Highly oxidized

states Mn^{6+} and Mn^{7+} can even be seen on the surface of LSMO film annealed in oxygen. Mn valence states on the films surface are discussed with the magnetic properties of LSMO films.

2. Experimental

LSMO films were prepared on STO (001) single-crystal substrates at 973 K by PLD. A KrF excimer laser (the wavelength is 248 nm) operating at about 2 J/cm^2 was focused on the surfaces of a rotating LSMO target. STO substrates were placed on a heater, which was 50 mm away from the target. The working pressure of O_2 flow during the deposition was maintained at 30 Pa. As-prepared LSMO samples with same deposition conditions were annealed at 973 K for 1 hours in flowing oxygen at atmospheric pressure (in a tube furnace) and in high vacuum (~1.0×10^{-5} Pa in the PLD chamber), respectively.

The crystalline structure of LSMO films was analyzed by an X-ray diffractometer (Bruker, D8 Discover) with Cu K_α radiation (λ = 0.15405 nm). The magnetization vs magnetic filed (*M-H*) curves were measured by using a commercial physical property measurement system (Quantum Design, PPMS). The thickness of LSMO films was indirectly tested by comparing with the corresponding thicker films (above 500 nm) measured by a surface profiler (Taylor Honson, S4C-3D). XPS experiments were carried out on an X-ray photoelectron spectrometer (Thermo Scientific, VG Multilab 2000) with Al Kα radiation (*hv*=1486.6 eV) under UHV (1.33×10^{-8} Pa). The energy resolution was set to 0.5 eV for wide scans and 0.05 eV for narrow scans, respectively. The analyzer pass energy was set to 40 eV for narrow scans. All peaks are calibrated by the carbon deposit C1s binding energy at 284.8 eV.

3. Results and Discussion

XRD pattern in Fig. 1 shows that only (00*l*) diffraction peaks of the as-prepared LSMO film are observed. No other peaks can be detected, which indicates that high quality LSMO films are orientated on STO substrates. After annealing, there are no detectable changes in XRD patterns (not shown). XPS wide scans also indicate that the stoichiometric ratios of the LSMO films did not changed much after annealing (see Fig. 2). The thicknesses of LSMO films are all controlled at about 100 nm by the laser pulses during the preparation.

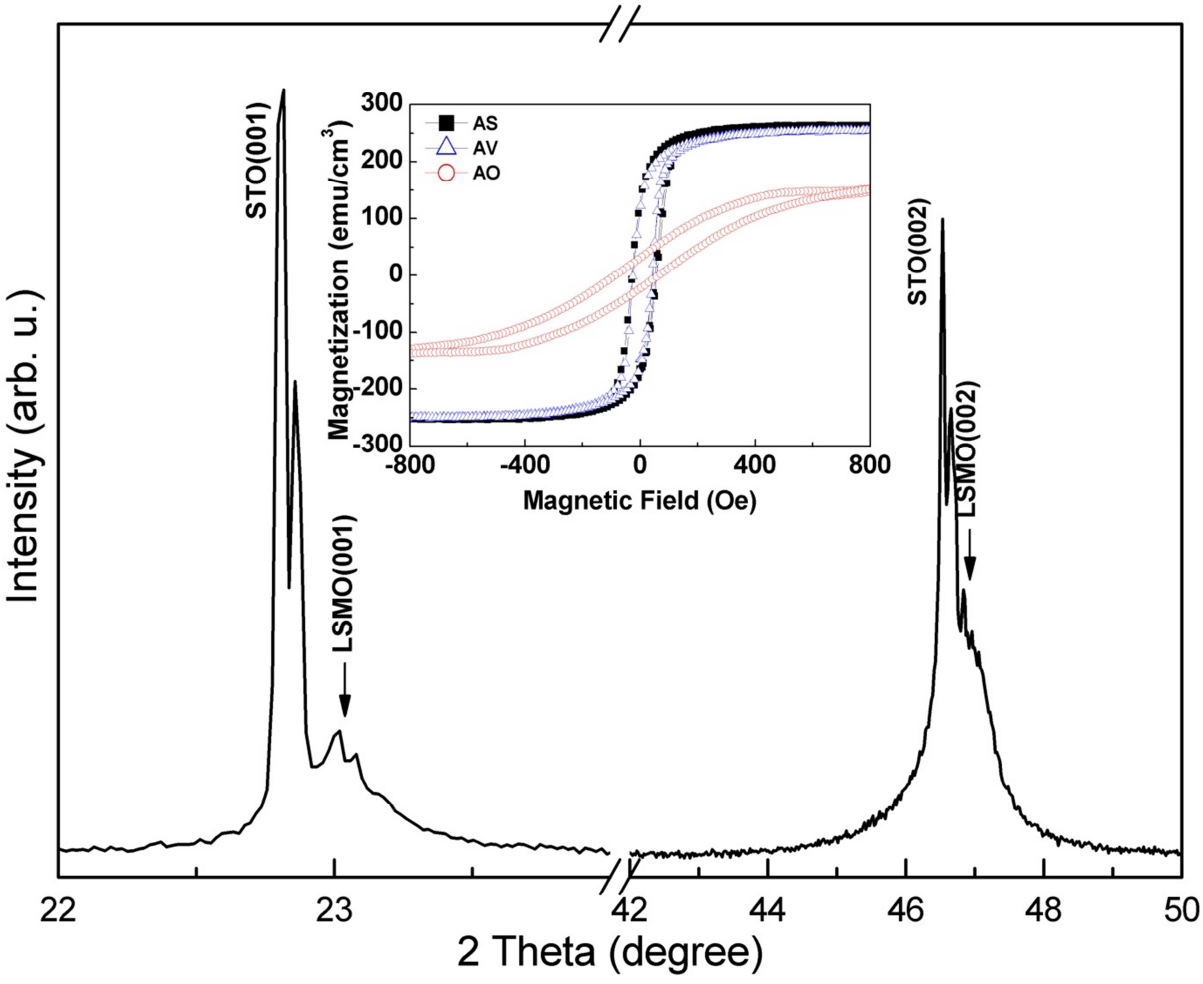

Fig. 1. *XRD pattern of the as-prepared LSMO film. Inset is M-H curves of LSMO films under various post-deposition treatments: as-prepared (AS), annealed in vacuum (AV) and annealed in oxygen (AO). M-H curves were measured at room temperature.*

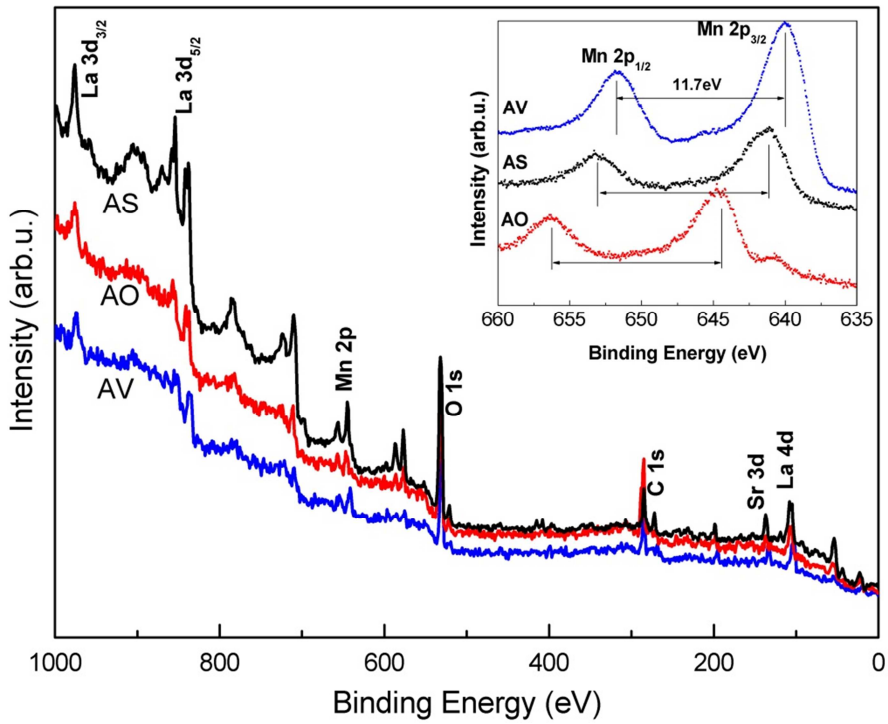

Fig. 2. *XPS wide spectra of LSMO films for as-prepared (AS), annealed in oxygen (AO) and annealed in vacuum (AV). Inset: Mn 2p spectra of LSMO films: annealed in vacuum (AV), as-prepared (AS) and annealed in oxygen (AO).*

The inset in Fig. 1 shows that the coercive forces are about 35 Oe, which is attributed to the high quality and low defect density of epitaxial LSMO films on STO substrates [16]. H. Boschker reported the coercive forces (25~100 Oe) of LSMO thin films with different film thickness and substrate surface [17].

The inset in Fig. 2 shows the Mn 2p photoelectron spectra of the LSMO films. For the as-prepared LSMO film, a broad doublet emission line between 635 eV and 658 eV can be seen, which is agreed with the reports [14, 15, 18]. Two maxima (around 641.4 eV and 653.1 eV) can be assigned to $2p_{3/2}$ and $2p_{1/2}$ states, respectively. There are also broad doublet emission lines in the annealed films, which shift to lower energy side and higher energy side, respectively. The values of the Mn 2p splitting in these LSMO films are all about 11.7 eV.

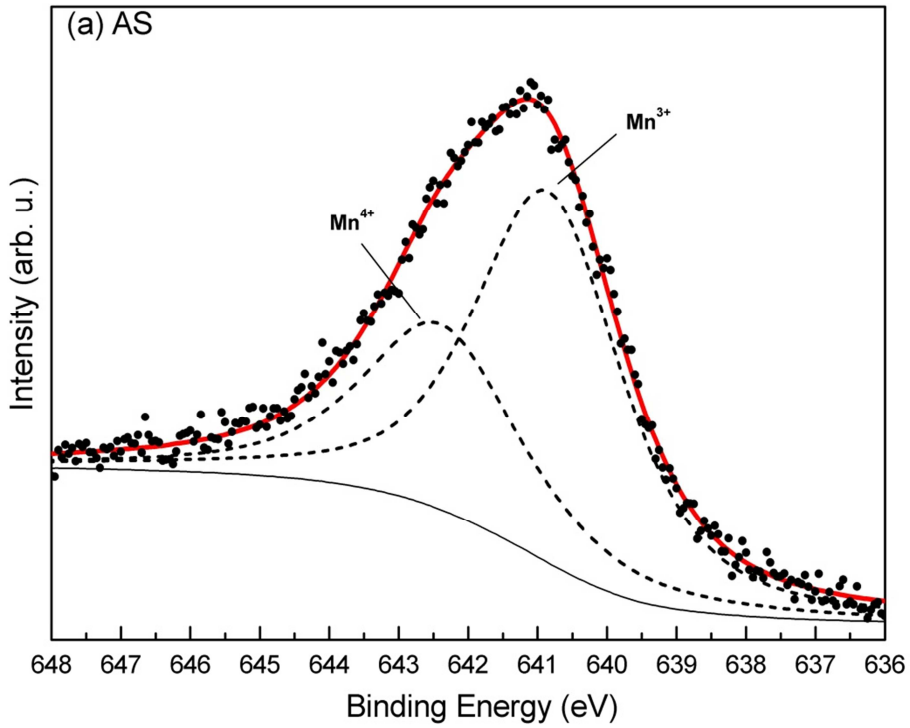

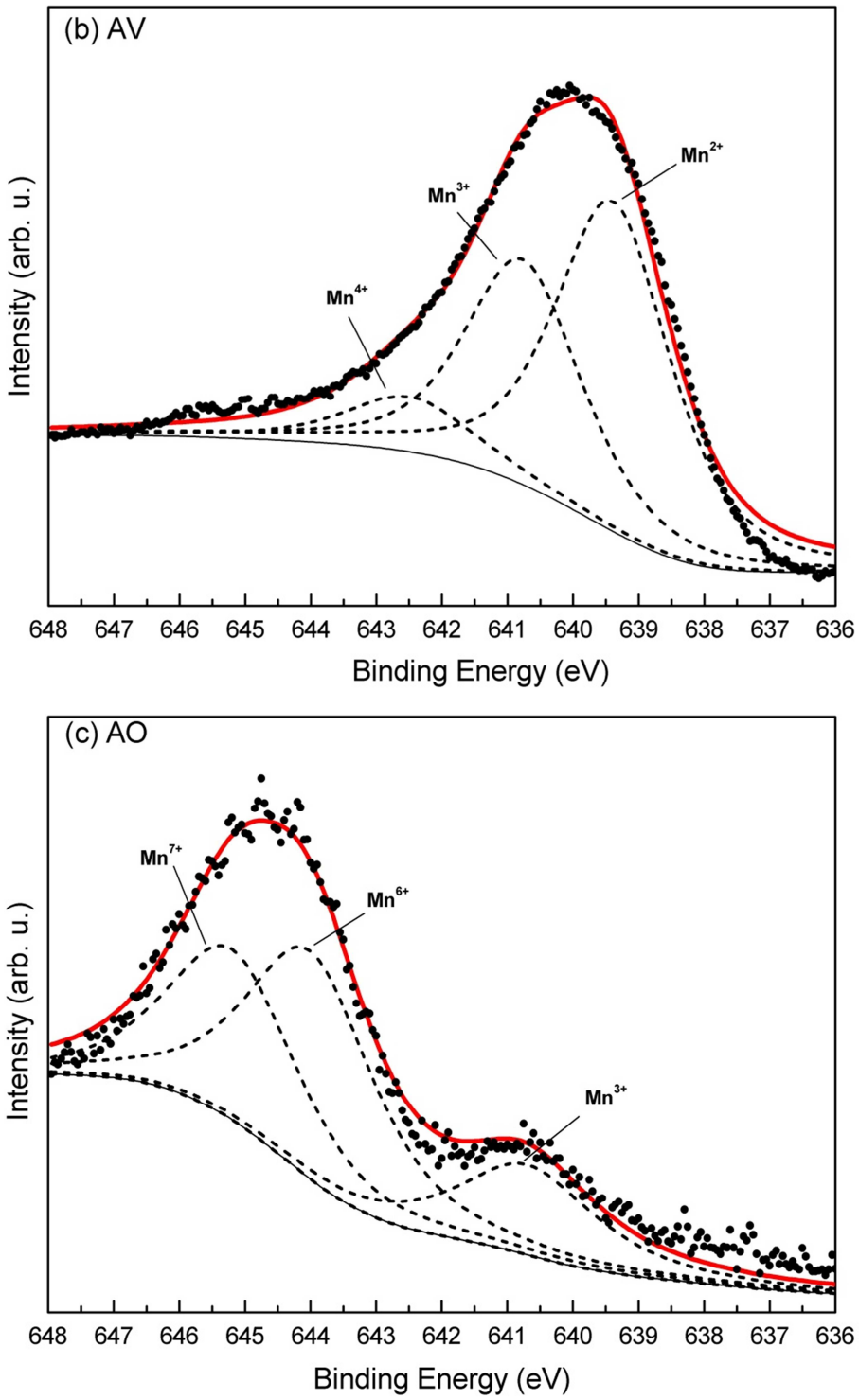

Fig. 3. *Mn $2p_{3/2}$ spectra of LSMO films for as-prepared (a), annealed in vacuum (b) and annealed in oxygen (c). Circle dots represent the spectra data, thick solid lines are Mn ($2p_{3/2}$) spectral fittings, thin solid lines are backgrounds.*

Mn $2p_{3/2}$ spectra were fitted as shown in Fig. 3. Spectra were analyzed using the PEAKFIT 4.0 software. A standard Shirley background is used for all spectra. The FWHM values of all peaks are set as 2.5~2.7 eV. The peak shapes are all kept as 70% Gaussian-30% Lorentzian. Since there could be more complex valence states in film materials than that of quality bulk samples, spectra fittings can not do as well as that of bulk samples. The peak centers of Mn^{2+}, Mn^{3+}, Mn^{4+}, Mn^{6+} and Mn^{7+} are around 639.4, 640.8, 642.4, 644, and 645.2 eV, respectively [13, 14, 18].

The percentages of total area of peaks after spectra fitting are calculated. The ratio of Mn^{3+}/Mn^{4+} is about 1.86 on the surface of the as-prepared LSMO film, which is nearly equal to Mn^{3+}/Mn^{4+} (about 2) in the stoichiometric $La_{0.67}Sr_{0.33}MnO_3$ material. After the film annealed in vacuum, the ratio of Mn^{3+}/Mn^{4+} on the film surface increases to about

3. Since XPS measurements only confirm the surface condition and considering the nearly unchanged *M-H* curves (see inset in Fig. 1), it can deduce that Mn^{3+}/Mn^{4+} remains at 2 in the film annealed in vacuum.

Jong et al. reported an increase of Mn^{2+} in $La_{0.7}Sr_{0.3}MnO_3$ films from the resonant photoemission (RPE) measurements after deoxygenating treatments in vacuum, which was connected with Mn^{2+} ions close to oxygen vacancies mainly formed at surface defects [15]. Here Mn^{2+} on the surface of the films annealed in vacuum might due to the deoxygenating process. Films deposited by PLD usually have low defects. In practice, nearly oxygen stoichiometric LSMO films can be obtained for oxygen pressures above 25 Pa during the deposition [19, 20]. The magnetic property of LSMO is originated from Mn^{3+}-O-Mn^{4+} double exchange interaction [21]. As nonferromagnetic ions [15], Mn^{2+} has little effect on M_s of LSMO films.

Fig. 3(c) shows that Mn^{4+} nearly disappeared on the surface of LSMO film annealed in oxygen. Considering the decreased magnetic property (see inset in Fig. 1), we can deduce the contents of Mn^{3+} and Mn^{4+} also changed in the interior of LSMO film after annealing in oxygen, though it can not be seen from the XRD pattern. Because the double exchange interaction between pairs of Mn^{3+} and Mn^{4+} ions is responsible for the ferromagnetic properties in LSMO [15, 16, 21].

For the film annealed in oxygen, Mn^{6+} and Mn^{7+} states can be seen. Although annealing can improve crystallization, epitaxial LSMO films as-deposited by PLD have well-crystallized [12, 16, 22]. So no improvements in the magnetic properties can be seen from *M-H* curves after annealing. On the other hand, high oxygen partial pressure can sweep off oxygen vacancies and Mn^{2+}, and then even oxidize Mn ions into higher valence states. The disproportionate Mn^{3+}/Mn^{4+} in the film annealed in oxygen can be related to the lower saturation magnetization of LSMO films.

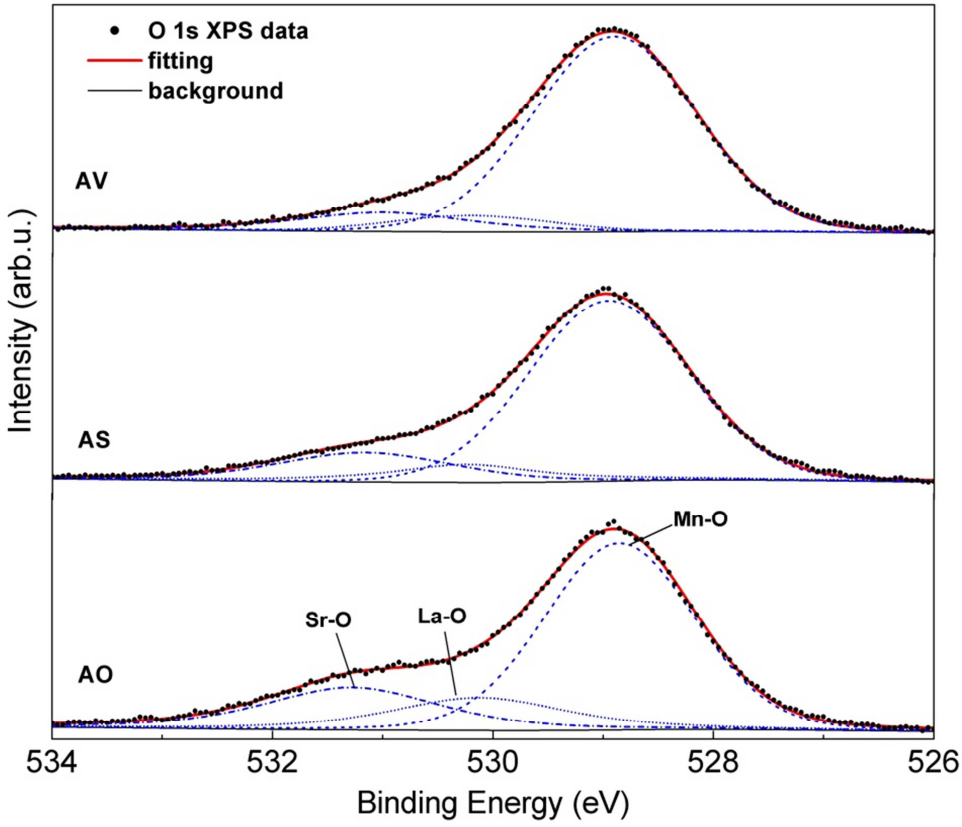

Fig. 4. *O 1s spectra of LSMO films for annealed in vacuum (AV), as-prepared (AS), and annealed in oxygen (AO). Circle dots represent the spectra data, thick solid lines are Mn ($2p_{3/2}$) spectral fittings and thin solid lines are backgrounds.*

Fig. 4 shows O 1s spectra, in which every spectrum was deconvoluted into three peaks. The positions of the three peaks are around 529, 530.2, and 531.3 eV, which are associated with Mn-O, La-O and Sr-O, respectively [23]. It can be seen that the ration of Mn-O is biggest on the surface of LSMO film annealed in vacuum. La-O and Sr-O increase after the film annealed in oxygen, which indicate that the somewhat segregation of Sr might occur on the surface [23].

4. Conclusion

Orientated LSMO films prepared by PLD were annealed in oxygen and vacuum, respectively, which show apparently peak-shifting Mn 2p XPS spectra and changed magnetic properties. Multiple peaks fitting for Mn $2p_{3/2}$ shows that Mn^{3+}/Mn^{4+} increase and Mn^{2+} appears on the surface after the as-prepared film annealed in high vacuum. The saturation

magnetization remains unchanged indicates Mn^{3+}/Mn^{4+} in the film changed little. For the LSMO film annealed in oxygen, high oxygen partial pressure can sweep off Mn^{2+} and even oxidize Mn ions into higher valence states, which changes Mn^{3+}/Mn^{4+} and decreases the saturation magnetization.

Acknowledgement

We are grateful to the National Natural Science Foundations of China (nos. 51272072).

References

[1] V. Garcia, M. Bibes, L. Bocher, et al., Ferroelectric control of spin polarization, Science 327 (2010) 1106.

[2] G. Kim, D. Mazumdar, A. Gupta, Nanoscale electroresistance properties of all-oxide magneto-electric tunnel junction with ultra-thin barium titanate barrier, Appl. Phys. Lett. 102 (2013) 052908.

[3] Z. H. Wang, W. S. Zhao, W. Kang, et al., Write operation study of Co/BTO/LSMO ferroelectric tunnel junction, J. Appl. Phys. 114 (2013) 044108.

[4] H. J. Mao, C. Song, L. R. Xiao, et al., Unconventional resistive switching behavior in ferroelectric tunnel junctions, Phys. Chem. Chem. Phys. 17 (2015) 10146-10150.

[5] L. Akaslompolo, A. M. Sánchez, Q. H. Qin, et al., Structural and magnetic properties of pulsed laser deposited $SrRuO_3/CoFe_2O_4$ $/La_{2/3}Sr_{1/3}MnO_3$ magnetic oxide heterostructures on $SrTiO_3$ (001) and MgO (001), Appl. Phys. A, 110 (2013) 889–894.

[6] A. Vailionis, H. Boschker, Z. Liao, et al., Symmetry and lattice mismatch induced strain accommodation near and away from correlated perovskite interfaces, Appl. Phys. Lett. 105 (2014) 131906.

[7] A. Kumar, D. Barrionuevo, N. Ortega, et al., Ferroelectric capped magnetization in multiferroic PZT/LSMO tunnel junctions, Appl. Phys. Lett. 106 (2015) 132901.

[8] M. Huijben, Y. H. Liu, H. Boschker, et al., Enhanced local magnetization by interface engineering in perovskite-type correlated oxide heterostructures, Adv. Mater. Interfaces 2 (2015) 1400416.

[9] D. R. Sahua, D. K. Mishra, J. L. Huang, et al., Annealing effect on the properties of $La_{0.7}Sr_{0.3}MnO_3$ thin film grown on Si substrates by DC sputtering, Physica B, 396 (2007) 75-80.

[10] H. P. Xie, H. Huang, N. T. Cao, et al., Effects of annealing on structure and composition of LSMO thin films, Physica B, 477 (2015) 14-19.

[11] H. W. Nesbitt, D. Banerjee, Interpretation of XPS Mn (2p) spectra of Mn oxyhydroxides and constraints on the mechanism of MnO_2 precipitation, Am. Mineral. 83 (1998) 305–315.

[12] H. Boschker, M. Huijben, A. Vailionis, et al., Optimized fabrication of high-quality $La_{0.67}Sr_{0.33}MnO_3$ thin films considering all essential characteristics, J. Phys. D: Appl. Phys. 44 (2011) 205001.

[13] M. C. Biesinger, B. P. Payne, A. P. Grosvenor, et al., Resolving surface chemical states in XPS analysis of first row transition metals, oxides and hydroxides: Cr, Mn, Fe, Co and Ni, Appl. Surf. Sci., 257 (2011) 2717–2730.

[14] M. P. de Jong, I. Bergenti, V. A. Dediu, et al., Evidence for Mn^{2+} ions at surfaces of $La_{0.7}Sr_{0.3}MnO_3$ thin films, Phys. Rev. B 71 (2005) 014434.

[15] M. P. de Jong, I. Bergenti, W. Osikowicz, et al., Valence electronic states related to Mn^{2+} at $La_{0.7}Sr_{0.3}MnO_3$ surfaces characterized by resonant photoemission, Phys. Rev. B 73 (2006) 052403.

[16] D. Liu, W. Liu, Growth and characterization of epitaxial $(La_{2/3}Sr_{1/3})$ MnO_3 films by pulsed laser deposition, Ceram. Inter. 37 (2011) 3531–3534.

[17] H. Boschker, M. Mathews, P. Brinks, et al., Uniaxial contribution to the magnetic anisotropy of $La_{0.67}Sr_{0.33}MnO_3$ thin films induced by orthorhombic crystal structure, J Mag. Mag. Mater. 323 (2011) 2632–2638.

[18] T. Hishida, K. Ohbayashi, T. Saitoh, Hidden relationship between the electrical conductivity and the Mn 2p core-level photoemission spectra in $La_{1-2x}Sr_xMnO_3$, J Appl. Phys. 113 (2013) 043710.

[19] M. Cesaria, A. P. Caricato, G. Leggieri, et al., Optical response of oxygen deficient $La_{0.7}Sr_{0.3}MnO_3$ thin films deposited by pulsed laser deposition, Thin Solid Films 545 (2013) 592–600.

[20] Z. Li, M. Bosman, Z. Yang, et al., Interface and surface cation stoichiometry modified by oxygen vacancies in epitaxial manganite films, Adv. Funct. Mater. 22 (2012) 4312.

[21] C. Zener, Interaction between the d-shells in the transition metals. II. Ferromagnetic compounds of manganese with perovskite structure, Phys. Rev. 82 (1951) 403.

[22] A. Goktas, F. Aslan, I. H. Mutlu, Annealing effect on the characteristics of $La_{0.67}Sr_{0.33}MnO_3$ polycrystalline thin films produced by the sol-gel dip-coating process, J. Mater. Sci.: Mater. Electron 23 (2012) 605–611.

[23] P. Decorse, E. Quenneville, S. Poulin, et al., Chemical and structural characterization of $La_{0.5}Sr_{0.5}MnO_3$ thin films prepared by pulsed-laser deposition, J. Vac. Sci. Technol. A 19 (2001) 910-915.